Synthesis of Conformationally Restricted Carbocyclic Nucleosides: The Role of the O(4′)-Atom in the Key Hydration Step of Adenosine Deaminase

by **Victor E. Marquez**[a])*, **Pamela Russ**[a]), **Randolph Alonso**[a]), **Maqbool A. Siddiqui**[a]), **Susana Hernandez**[a]), **Clifford George**[b]), **Marc C. Nicklaus**[a]), **Fang Dai**[a]), and **Harry Ford, Jr.**[a])

[a]) Laboratory of Medicinal Chemistry, Division of Basic Sciences, National Cancer Institute, National Institutes of Health, Bethesda, MD 20892, USA

[b]) Laboratory for the Structure of Matter, Naval Research Laboratory, Washington, DC 20375, USA

Dedicated to Prof. Dr. *Frank Seela* on the occasion of his 60th birthday

Conformationally restricted carbocyclic nucleosides with either a northern(*N*)-type conformation, *i.e.*, *N*-type 2′-deoxy-methanocarba-adenosine **8** ((*N*)MCdAdo), or a southern(*S*)-type conformation, *i.e.* *S*-type 2′-deoxy-methanocarba-adenosine **9**, ((*S*)MCdAdo), were used as substrates for adenosine deaminase (ADA) to assess the enzyme's preference for a fixed conformation relative to the flexible conformation represented by the carbocyclic nucleoside aristeromycin (**10**). Further comparison between the rates of deamination of these compounds with those of the two natural substrates adenosine (Ado; **1**) and 2′-deoxyadenosine (dAdo; **2**), as well as with that of the conformationally locked nucleoside LNA-Ado (**11**), which, like the natural substrates, has a furanose O(4′) atom, helped differentiate between the roles of the O(4′) anomeric effect and sugar conformation in controlling the rates of deamination by ADA. Differences in rates of deamination as large as 10000 can be attributed to the combined effect of the O(4′) atom and the enzyme's preference for an *N*-type conformation. The hypothesis proposed is that ADA's preference for *N*-type substrates is not arbitrary; it is rather the direct consequence of the conformationally dependent O(4′) anomeric effect, which is more efficient in *N*-type conformers in promoting the formation of a covalent hydrate at the active site of the enzyme. The formation of a covalent hydrate at the active site of ADA precedes deamination. A new and efficient synthesis of the important carbobicyclic template **14a**, a useful intermediate for the synthesis of (*N*)MCdAdo (**8**) and other conformationally restricted nucleosides, is also reported.

Introduction. – Adenosine deaminase (ADA, EC 3.5.4.4) is a critical enzyme of the purine metabolic pathway that catalyzes the irreversible hydrolytic deamination of adenosine (Ado; **1**) and 2′-deoxyadenosine (dAdo; **2**) – as well as of other exogenous substrates – to their hypoxanthine derivatives **4** and **5**, respectively, and ammonia (*Scheme 1*) [1][2]. Aberrations in the expression and function of ADA have been associated with impaired B- and T-cell-based immunity, whereas elevated levels of ADA have been observed in certain lymphomas and leukemias [3–5]. Thus, a complete understanding of the ADA-catalyzed mechanism of deamination should provide additional means of intervening therapeutically in ADA-related disorders. The rational design of the first transition-state analogue inhibitor of ADA by *Wolfenden* and *Evans* in 1970 [6] was followed four years later by the discovery of the potent fermentation-product inhibitors coformycin (**6**) [7][8] and 2′-deoxycoformycin (**7**) [9], which were shown to function as stable, high-affinity transition-state-analogue inhibitors of ADA [10][11]. Further confirmation of the transition-state mimicry of these analogues came from several crystal structures of ADA with the ligands bound at the active site of the enzyme [12–14]. In the case of the simple purine riboside **3**

(nebularine), covalent hydration at the active site of ADA is able to generate the potent transition-state inhibitor (6*S*)-1,6-dihydro-9*H*-purin-6-ol riboside **3a** [11] (*Scheme 1*). However, since the equilibrium constant for this critical hydration step is very small, the apparent inhibition constant of nebularine is only in the micromolar range [11]. On the other hand, the transition-state inhibitors coformycin (**6**) and 2′-deoxycoformycin (**7**), where the 8-hydroxy substituent of the diazepine ring provides a stable mimic of a hydrated ring, are able to inhibit ADA at picomolar levels [10][11]. From these observations, it was concluded that all ADA substrates must form a covalent hydrate (*i.e.* **1a** and **2a** in *Scheme 1*) as a first critical step before deamination. Calculation of relative hydration free energy differences in heteroaromatic bases have revealed the importance of electronic and steric factors in facilitating hydration of the aglycon as a key step in the deamination reaction [15]. For example, a comparison between nebularine (**3**) and its 8-aza analogue showed a 400-fold greater ADA inhibitor potency for the latter, which is attributable to the enhancing effect of hydration caused by the N-atom at the 8-position [15]. The role of the sugar moiety in this key hydration step, on the other hand, has for the most part been ignored and even considered negligible [15]. In the present work, we wish to address this issue by comparing the deamination rates of substrates that differ from Ado and dAdo in that the furanose ring has been replaced by a cyclopentane ring.

Scheme 1

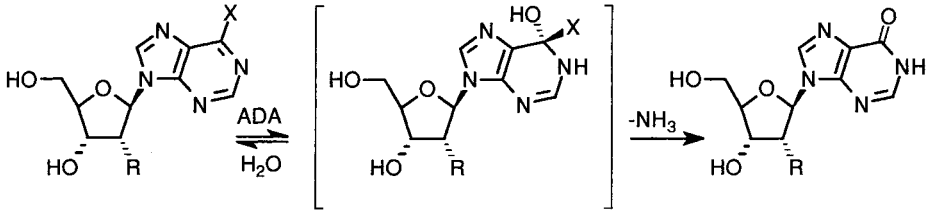

1 X = NH_2, R = OH (Ado) → **1a** X = NH_2, R = OH (transition state) → **4** R = OH (inosine)
2 X = NH_2, R = H (dAdo) → **2a** X = NH_2, R = H (transition state) → **5** R = H (2′-deoxyinosine)
3 X = H, R = OH (nebularine) → **3a** X = H, R = OH (unproductive complex)

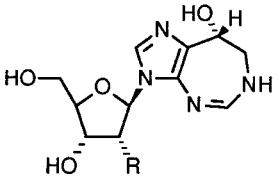

6 R = OH (coformycin)
7 R = H (2′-deoxycoformycin)

In addition, since ADA-inhibitor complexes [12–14] have revealed a preferred northern(*N*)-type conformation for the bound inhibitor at the active site – and by extension one can assume that substrates will bind with the same preferred conformation – we have chosen to study the deamination rates of carbocyclic adenosine nucleosides locked in antipodal conformations (northern(*N*)- and southern-

(*S*)-type) similar to those of the furanose ring, as defined by the pseudorotation phase angle *P* [16]. Normally, conventional nucleosides in solution undergo rapid equilibration between ranges of *P* defined by two main furanose puckering domains centered around a $^3T_2$ (*N*-type) and a $^2T_3$ (*S*-type) conformation (*Fig. 1*). These conformational modes, in turn, favor particular orientations of the glycosyl torsion angle χ (*syn* or *anti*) and the 4-(hydroxymethyl) chain defined by γ (+*sc*, − *sc*, and *ap*). Indeed, the range of values of χ and γ are not uniformly populated, and their preferred distribution is coupled to a particular sugar pucker [17]. The conformationally locked carbocyclic adenosine substrates selected for this study were (*N*)MCdAdo (**8**), as a rigid *N*-type conformer, and (*S*)MCdAdo (**9**) as a rigid *S*-type conformer. The fermentation product aristeromycin (Ari; **10**) was used as a base-line reference for a flexible, carbocyclic nucleoside substrate. Indeed, aristeromycin has been shown to undergo rapid equilibration in solution between a southwestern-type and an *N*-type conformer, with a bias towards the former [18]. Comparison between the rates of deamination of these compounds with those of the two natural substrates Ado (**1**) and dAdo (**2**), as well as with that of the conformationally locked nucleoside LNA-Ado (**11**) [19], helped differentiate the roles of the O(4′) atom's anomeric effect and sugar conformation in controlling the rates of deamination by ADA. As in the natural substrates, the conformationally locked nucleoside LNA-Ado has a O(4′) furanose atom, and its enhanced rate of deamination relative to the conformationally locked carbocyclic nucleosides highlights the importance of the anomeric effect contributed by the O(4′) atom.

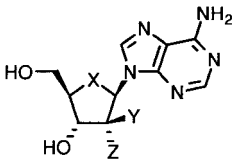

1 X = O, Y = H, Z = OH (Ado)
2 X = O, Y = Z = H (dAdo)
10 X = CH_2, Y = H, Z = OH (Ari)

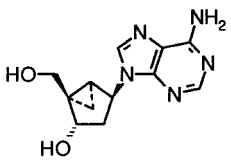

8 (*N*)MCdAdo

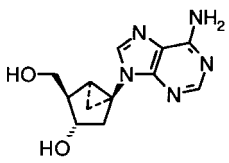

9 (*S*)MCdAdo

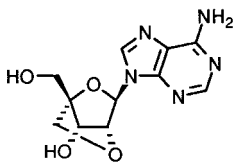

11 LNA-Ado

In this work, we also wish to present a new and more efficient six-step synthesis of the critical precursor **14a**, which is an extremely useful intermediate for the convergent synthesis of (*N*)MCdAdo and other *N*-type purine analogues. The overall yield of 35% obtained for **14a** compares favorably with our previous seven-step synthesis reported earlier (25% yield) [20].

Results. – *Synthesis and Structural Analysis of Carbocyclic Nucleosides.* The syntheses of the conformationally locked *N*-type nucleoside (*N*)MCdAdo (**8**), as well

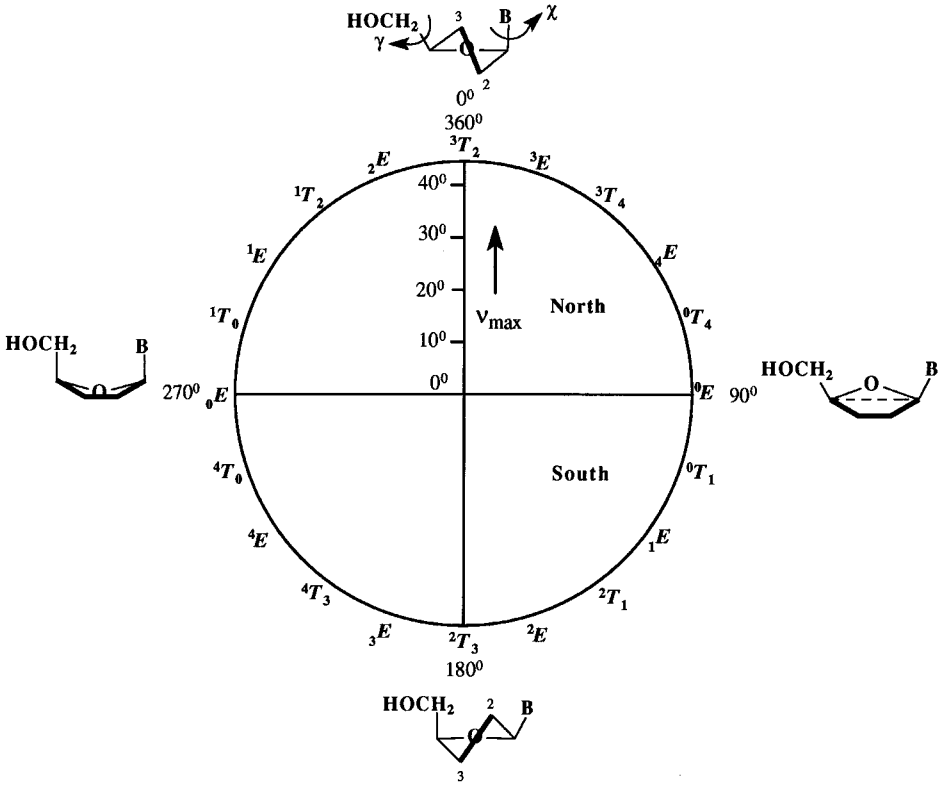

Fig. 1. *Pseudorotational cycle displaying all the puckering modes* (P) *and maximum puckering amplitude* (ν_{max})

as that of the *S*-type analogue (*S*)MCdAdo (**9**), have been reported [20][21]. While the X-ray structure of (*N*)MCdAdo (**8**) was published in conjunction with its synthesis [20][1]), we now report for the first time the crystal structure of (*S*)MCdAdo (**9**)[2]). From comparing the two structures, it is clear that these carbocyclic nucleosides adopt fixed conformations that mimic the ring pucker of a furanose ring (*Figs. 2* and *3*). As discussed in a preliminary communication [22], the crystallographic pseudorotational parameters for the two molecules (A and B) in the unit cell of (*N*)MCdAdo are in complete agreement with the expected values for a *N*-type ($_2E$) conformation ($P=$ 342.78° (A) and $P=339.25°$ (B)), whereas the equivalent parameters for the antipodal (*S*)MCdAdo correlate with a pure *S*-type ($_3E$) conformation ($P=199.10°$ (A) and $P=200.20°$ (B)). Except for the molecule A of (*S*)MCdAdo, all torsion angles χ are in the *anti* range, while the less encumbered angle γ alternates between the *ap* and $+sc$ conformations as it is normally seen in conventional nucleosides [22].

---

[1]) *CCDC* entry NAKZUU.

[2]) Crystallographic data have been deposited with the *Cambridge Crystallographic Data Centre* as deposition No. CCDC-133070. Copies of the data can be obtained, free of charge, by applying to the *CCDC*, 12 Union Road, Cambridge CB2 1EZ, UK (fax: + 44(0)1223-336033; e-mail: deposit@ccdc.com.oc.uk).

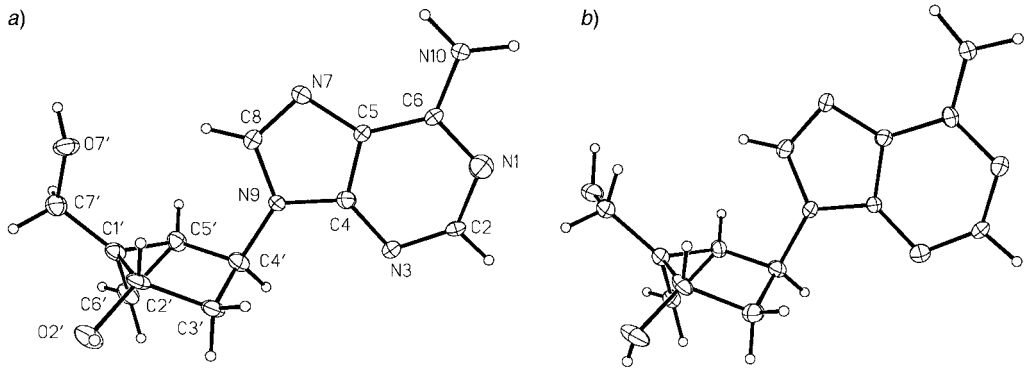

Fig. 2. *Molecular structure of* (N)*MCdAdo* (**8**)*:* a) *molecule A* ($\chi = -154.8°$ (*anti*), $\gamma = +54.8°$ (+*sc*)) *and* b) *molecule B* ($\chi = -167.6°$ (*anti*), $\gamma = -177.6°$ (*ap*))

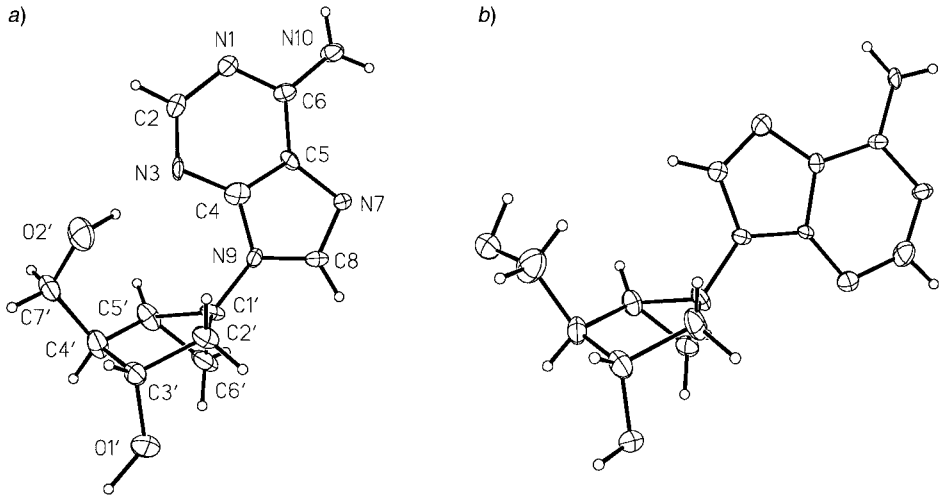

Fig. 3. *Molecular structure of* (S)*MCdAdo* (**9**): a) *molecule A* ($\chi = +50.9°$ (*syn*), $\gamma = +54.0°$ (+*sc*)) *and* b) *molecule B* ($\chi = -129.8°$ (*anti*), $\gamma = -171.9°$ (*ap*))

The new approach to the synthesis of (*N*)MCdAdo (**8**) was based on the easily available chiral template (3*R*,4*S*)-4-(phenylmethoxy)-3-[(phenylmethoxy)methyl]cyclopent-1-ene (**12**) [23–25]. This approach compared favorably with respect to the one devised earlier from chiral cyclopentenone **13** [20], particularly in the generation of the key carbobicyclic intermediates **14a**,**b** (*Scheme 2*). In the same manner as reported previously with the PhSeCl/NaN_3 system [25], the double bond in **12** reacted regio- and stereoselectively with PhSeCl/$AgCF_3CO_2$ to give the *trans*-2-(phenylseleno)cyclopentan-1-ol intermediate **15** after hydrolysis of the trifluoroacetate ester (*Scheme 3*). Following oxidation of the (phenylseleno) group, unidirectional elimination of PhSeOH gave exclusively the corresponding allylic alcohol **16**. This allylic alcohol was inverted following a *Mitsunobu* esterification which gave the intermediate benzoate **17** and the new allylic alcohol **18** after ester hydrolysis. Finally, a hydroxy-

Scheme 2

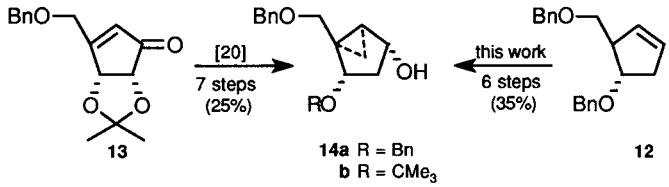

Scheme 3

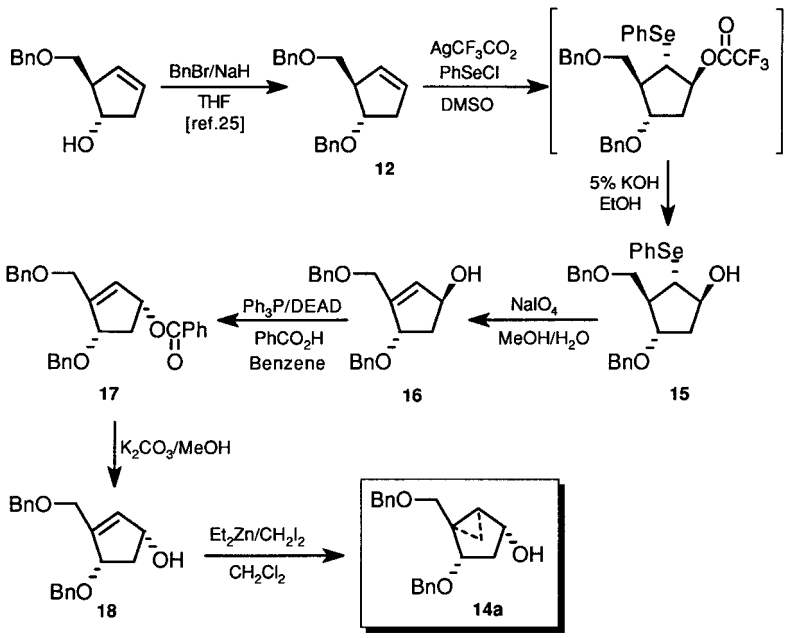

directed cyclopropanation under *Simmons-Smith* conditions gave the key carbobicyclic intermediate **14a** in 35% overall yield. This process required one step less than the previously reported approach [20] and provided a 10% increase in the overall yield of the final product. The synthesis of (*N*)MCdAdo (**8**) from **14a** proceeded essentially as reported before from intermediate **14b** [20], *i.e., via* **19** and **20** (*Scheme 4*).

The conformationally locked, pentofuranose-containing LNA-Ado (**11**), the synthesis of which has been reported earlier [19], was a kind gift from Professor *Wengel*. On conformational grounds, however, the locked 2,5-dioxabicyclo[2.2.1]heptane system does not have the same type of ring pucker as the bicyclo[3.1.0]hexane. The reported X-ray structure of the corresponding LNA-uracil analogue [26] shows that the 2,5-dioxabicyclo[2.2.1]heptane system has a *P* value of 17.4°, which is *ca.* 34–38° away from the pseudorotational angle of the locked *N*-type bicyclo[3.1.0]hexane template of carbocyclic nucleoside **8**. These different envelope conformations, ${}_2E$ *vs.* ${}^3E$ (see *Fig. 1*), could account for some differences in the rates of deamination discussed below.

Scheme 4

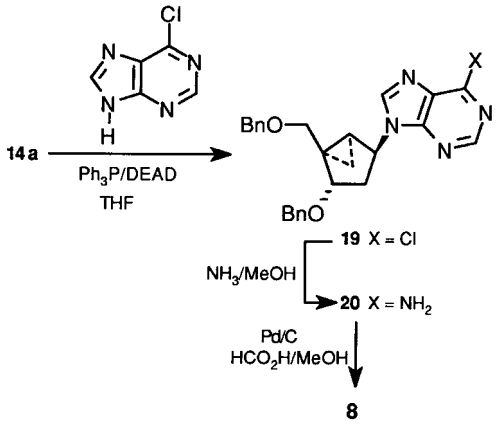

Adenosine Deaminase Activity. The compounds listed in the *Table* can be grouped in two categories depending on their substrate properties. The first three substrates **1**, **2**, and **11** fall in the category of good substrates, as indicated by the various kinetic parameters such as K_m, K_{cat}, and the catalytic efficiency (K_{cat}/K_m). The difference between these substrates and the carbocyclic analogues as a group appears substantial in view of the relative hydrolysis rates measured at 50 μM substrate concentration. Despite the poor deamination rates among the locked carbocyclic analogues **8**–**10**, there appears to be a clear preference for the *N*-type conformation. This observation is in agreement with the published X-ray structures of ADA-inhibitor complexes where the sugar moieties of the nucleosides bound at the active site appear puckered as *N*-type sugars [12–14]. Interestingly, the rate of deamination of the conformationally flexible aristeromycin (**10**) lies between the rates of deamination of the rigid *N*-type (*N*)MCdAdo (**8**) and the rigid *S*-type (*S*)MCdAdo (**9**) analogues. Obviously, the carbocyclic nucleosides are in a class by themselves as poor substrates of ADA, which appears to be a direct consequence of lacking the furanose O-atom. It has been clearly demonstrated by *Chattopadhyaya* and co-workers that the electronic nature of the aglycon is effectively transmitted to the pentofuranose moiety through the anomeric effect [27][28]. Indeed, the direct correlation of the protonation/deprotonation equilibrium of the aglycon with the two-state *N*/*S* pseudorotational equilibrium of the sugar moiety permits the facile calculation of the pK_a from the pD-dependent change of ΔG° in the *N*/*S* equilibrium [27][28]. On the other hand, a similar pK_a determination is not possible in carbocyclic nucleosides, and specifically for aristeromycin (**10**), because of the lack of the O(4′) atom and its associated anomeric effect [18][28]. Even though exact kinetic parameters between the two groups could not be compared, the differences in relative rates of deamination revealed some interesting trends worth discussing. For example, a direct comparison between the best ADA substrate, dAdo (**2**), and the best equivalent carbocyclic substrate, (*N*)MCdAdo (**8**), reveals a 122-fold difference in the rate of deamination in favor of the former that can be attributed to a combined effect of the O(4′) atom and the enzyme's preference for binding *N*-type substrates (*Table*). For the other two substrates, Ari (**10**) and

(*S*)MCdAdo (**9**), this difference can be even greater (200 and 10000, resp.). These larger differences are probably the result of higher energy penalties incurred for having a conformation far removed from the ideal *N*-type conformation. To gauge the conformational factor alone, a comparison between the rates of deamination of (*N*)MCdAdo (**8**) and (*S*)MCdAdo (**9**) would show the enzyme's capacity to effectively discriminate between the two rigid antipodal conformations. The nearly 100-fold difference between the rates of deamination of (*N*)MDdAdo (**8**) and (*S*)MCdAdo (**9**) demonstrates the enzyme's clear preference for an *N*-type conformer. In the real world, however, the effect of conformation is not as dramatic because of the nucleoside's inherent flexibility and capacity to adapt to the conformation demanded by the enzyme, something that would not be possible for (*N*)MDdAdo (**8**) and (*S*)MCdAdo (**9**). Indeed, Ado (**1**) and dAdo (**2**), which are known to exist in solution preferentially as *S*-type conformers [27], are expected to bind to the enzyme as *N*-type conformers [12–14]. From our study, it can be approximated that the combined anomeric effect of the O(4′) atom and the preference for an *N*-type conformation could account for differences in deamination rates as large as 10000. Since for nucleosides such as Ado (**1**) and dAdo (**2**), the anomeric effect is greater when the conformation of the sugar is of the *N*-type, the preference shown by ADA for *N*-type conformers is not a capricious preference; it results from the fact that in an *N*-type conformation, the anomeric effect stabilizes the protonated base more efficiently, a prerequisite for the formation of the covalent hydrate at the active site of ADA prior to deamination (*Scheme 1*) [11]. In these experiments, the dramatic effect of the O(4′) atom was revealed by its capacity to increase the rate of deamination of the conformationally locked nucleoside LNA-Ado (**11**) to *ca.* 20-fold relative to the best carbocyclic substrate (*N*)MCdAdo (**8**). This makes LNA-Ado only a 4-fold less efficient substrate than Ado (**1**). Such an increase in rate is clearly a direct consequence of the O(4′) atom's role in the critical hydration step prior to deamination. However, why did the rate of deamination of LNA-Ado (**11**) not match the level of deamination of Ado (**1**)? We have already discussed in the previous section that the X-ray structures of the locked 2,5-dioxabicyclo[2.2.1]heptane and the bicyclo[3.1.0]hexane systems used as *N*-type templates differ by 34–38° in pseudorotation (*P*). This 34–38° difference in *P* could account for the partial substrate recovery observed for LNA-Ado (**11**), as well as for the fact that there could be possible steric clashes at the receptor site between the structural elements added to constrain the rings and some critical amino-acid side chains. It must be remembered that, while there is a favorable entropic advantage in binding a constrained substrate, the enthalpy penalties could be rather severe when the fit is not perfect. It is possible, therefore, that while LNA-Ado (**11**) exists as an *N*-type conformer, it does not have the ideal conformation for a perfect fit. Despite this shortcoming, if one assumes that both conformationally rigid compounds, (*N*)MCdAdo (**8**) and LNA-Ado (**11**), approximate the preferred *N*-type conformation and are able to bind at the active site of ADA, the role of the O(4′) atom appears conclusive. Further confirmation of the importance of the O(4′) atom anomeric effect, as a critical determinant for the hydration step catalyzed by ADA and related enzymes, is found in the recent work of *Lindell* and co-workers who report that the 5′-monophosphate of the carbocyclic analogue of nebularine is a very poor inhibitor of the mechanistically equivalent adenosine 5′-monophosphate deaminase (AMPDA) [29].

Table. *Kinetic Constants for Various Substrates of ADA*[a])

	K_m [μM]	K_{cat} [s^{-1}]	K_{cat}/K_m [$\mu M^{-1}s^{-1}$]	Relative rate[b])
Ado (**1**)	33.1 ± 3.7	188	5.7	100
dAdo (**2**)	23.0 ± 2.3	245	10.6	121
LNA-Ado (**11**)	122 ± 12	59.4	0.49	19
(*N*)MCdAdo (**8**)	–	–	–	0.99
Ari (**10**)	–	–	–	0.58
(*S*)MCdAdo (**9**)	–	–	–	0.01

[a]) Kinetic constants were determined by UV at 37° and pH 7.4 with calf-intestine ADA. [b]) Relative rates were measured spectrophotometrically at 37° with 50 μM substrate concentration.

Experimental Part

1. *General*. All chemical reagents were commercially available. M.p.: *MelTemp-II* apparatus, *Laboratory Devices*, USA; uncorrected. Column flash chromatography (FC): silica gel *60* (230–400 mesh; *E. Merck*). ^{1}H- and ^{13}C-NMR Spectra: *Bruker-AC-250* instrument at 250 and 62.9 MHz, resp.; δ in ppm rel. to the solvent in which they were run (7.24 ppm for $CDCl_3$). Elemental analyses were performed by *Atlantic Microlab, Inc.*, Atlanta, GA.

2. *X-Ray Crystal Structure of (1*S*,3*S*,4*R*,5*S*)-1-(6-Amino-9*H*-purin-9-yl)-4-(hydroxymethyl)bicyclo[3.1.0]-hexan-3-ol* (**9**). *Crystal Data*[2]): $2(C_{12}H_{15}N_5O_2)\cdot 3(H_2O)$, M_r 576.63; crystal size: $0.40\times0.08\times0.02$ mm^3; monoclinic $P2_1$, $a=11.460(2)$ Å, $b=7.991(2)$ Å, $c=15.524(3)$ Å, $\alpha=90°$, $\beta=95.55(1)°$, $\gamma=90°$; $V=1377.9(5)$ Å^3, $Z=2$, $D_c=1.390$ mg/m^3, $\lambda(CuK_\alpha)=1.54178$ Å, $\mu=0.877$ mm^{-1}, $F(000)=612$, $T=293(2)$ K. Final *R* indices ($I>2\sigma(I_0)$) $R1=0.0658$, $wR2=0.1395$ for 2136 reflections. Tables of atomic coordinates, bond distances, and angles, and anisotropic thermal parameters have been deposited[2]).

3. *Kinetic Analysis and Adenosine Deaminase Assays.* Adenosine deaminase (calf intestine) activity was measured spectrophotometrically with a *Shimazdu-UV-PC-2101* spectrophotometer by following the disappearance of adenosine at 265 nm in 1-ml cuvettes with 0.1M phosphate (pH 7.4) at 25°. For the substrates listed in the *Table*, initial hydrolysis rates were determined by following the disappearance of substrate at 265 nm in 1-ml cuvettes with 0.1M phosphate (pH 7.4) at 37°. A similar molar extinction coefficient and a $\Delta\varepsilon=-7900$ was assumed for all adenine analogues examined. Kinetic constants were determined from *Lineweaver-Burk* plots with Graph-Pad Prism V 2.01 (*Graphpad Software*, *Inc.* San Diego, CA), a personal-computer-based curve-fitting program. A minimum of three determinations were performed. Relative-rate experiments were performed in duplicate using 50 μM substrate concentration at 37°.

4. *Syntheses. (3*R*,4*S*)-4-(Phenylmethoxy)-3-[(phenylmethoxy)methyl]cyclopent-1-ene* (**12**) was prepared in 95% yield as described in [25].

*(1*S*,4*S*)-4-(Phenylmethoxy)-3-[(phenylmethoxy)methyl]cyclopent-2-en-1-ol* (**16**). A mixture of **12** (2.36 g, 8.61 mmol) and phenylselenium chloride (1.98 g, 10.3 mmol) in dry DMSO (8 ml) was stirred under Ar at r.t. until solution occurred. Silver trifluoroacetate (2.28 g, 10.3 mmol) was added, and the mixture was stirred for 1 h. The mixture was then cooled over ice, and hydrolysis of the trifluoroacetate ester was accomplished with 5% KOH/EtOH (15 ml) while stirring for 0.25 h. The mixture was poured into ice-cold H_2O (100 ml) and extracted with Et_2O (3×100 ml), the combined Et_2O extract washed with sat. NH_4Cl soln. (35 ml), dried ($MgSO_4$), and evaporated, and the residue purified by FC (silica gel, step gradient of 10%, 20%, and 50% AcOEt/hexanes): reasonably pure *(1*S*,2*S*,3*R*,4*S*)-4-(phenylmethoxy)-3-[(phenylmethoxy)methyl]-2-(phenylseleno)cyclopentan-1-ol* (**15**; 2.98 g, 74%).

A mixture of crude **15** (2.20 g, 4.71 mmol) and $NaIO_4$ (2.02 g, 9.42 mmol) was stirred in MeOH/H_2O 9:1 (100 ml) for 1 h. After evaporation, the residue was stirred with AcOEt (100 ml), and the insoluble solid was removed by filtration. The filtrate was evaporated and the residue purified by FC (silica gel, step gradient of 25% and 50% AcOEt/hexanes): **16** (1.06 g, 73%). Clear oil. ^{1}H-NMR ($CDCl_3$): 7.44–7.30 (*m*, 2 Ph); 6.03 (br. *s*, H–C(2)); 5.10–5.04 (symmetrical *m*, H–C(1)); 4.90–4.84 (symmetrical *m*, H–C(4)); 4.67 (*AB*('*d*', $J=11.9$, 1 H, PhCH_2); 4.64 (*AB*('*d*'), $J=11.7$, 1 H, PhCH_2); 4.61 (*AB*('*d*'), $J=11.9$, 1 H, PhCH_2); 4.52 (*AB*('*d*'), $J=11.9$, 1 H, PhCH_2); 4.26 (br. *s*, $PhCH_2OCH_2$); 2.38 (*ddd*, $J=14.4, 6.8, 3.2$, H_a–C(5)); 2.09 (*ddd*, $J=14.1, 6.6, 3.2$, H_b–C(5)); 1.91 (br. *s*, OH). ^{13}C-NMR ($CDCl_3$): 145.54; 138.25; 138.03; 132.89; 128.25; 128.24; 127.57; 127.52;

127.48; 82.10; 75.28; 72.70; 71.28; 66.51; 41.16. Anal. calc. for $C_{20}H_{22}O_3 \cdot 0.25\ H_2O$ (314.89): C 76.27, H 7.21; found: C 76.40; H 7.28.

*(1*R*,4*S*)-4-(Phenylmethoxy)-3-[(phenylmethoxy)methyl]cyclopent-2-enyl Benzoate* (**17**). To a stirred soln. of **16** (1.06 g, 3.32 mmol) in dry benzene (50 ml), benzoic acid (0.63 g, 5.13 mmol) and Ph_3P (1.79 g, 6.84 mmol) were added. Diethyl azodicarboxylate (DEAD; 1.08 ml, 6.84 mmol) was added dropwise, and the reaction was allowed to continue at r.t. for 0.5 h. After all the volatiles were removed under reduced pressure, the residue was purified by FC (silica gel, 10% AcOEt/hexanes): **17** (1.27 g, 85%). Thick oil. ^{1}H-NMR ($CDCl_3$): 8.16–8.12, 7.67–7.34 (2*m*, 3 Ph); 6.17 (br. *s*, H–C(2)); 5.92–5.82 (symmetrical *m*, H–C(1)); 4.75–4.60 (*m*, 2 PhCH_2, H–C(4)); 4.35 (br. *s*, 2 H, PhCH_2OCH_2); 3.01 (*dt*, *J* = 14.2, 7.3, H_a–C(5)); 2.08 (*dt*, *J* = 14.4, 4.2, H_b–C(5)). ^{13}C-NMR: 166.46; 147.62; 138.48; 138.22; 133.07; 130.44; 129.82; 128.57; 128.55; 128.51; 128.47; 127.87; 127.85; 127.80; 80.80; 76.78; 73.11; 71.37; 66.73; 38.22. Anal. calc. for $C_{27}H_{26}O_4$ (414.50): C 78.24, H 6.32; found: C 78.40, H 6.72.

*(1*R*,4*S*)-4-(Phenylmethoxy)-3-[(phenylmethoxy)methyl]cyclopent-2-en-1-ol* (**18**). A stirred soln. of **17** (1.55 g, 3.59 mmol) in MeOH (50 ml) was treated with K_2CO_3 (1.24 g, 8.98 mmol). After 3 h, the solvent was evaporated and the residue purified by FC (silica gel, 5% MeOH/$CHCl_3$): **18** (0.874 g, 80%). Oil. ^{1}H-NMR ($CDCl_3$): 7.54–7.38 (*m*, 2 Ph); 6.03 (br. *s*, H–C(2)); 4.75–4.55 (*m*, 2 × PhCH_2O); 4.49–4.54 (*dd*, *J* = 6.8, 3.9, H–C(4)); 4.30 (br. *s*, PhCH_2OCH_2); 2.74 (*dt*, *J* = 14.2, 7.1, H_a–C(5)); 2.68 (br. *s*, OH); 1.82 (*dt*, *J* = 14.2, 3.9, H_b–C(5)); ^{13}C-NMR ($CDCl_3$): 144.86; 138.39; 138.20; 133.01; 128.44; 127.82; 127.78; 127.71; 80.99; 73.98; 72.84; 71.48; 66.62; 41.16. Anal. calc. for $C_{20}H_{22}O_3 \cdot 0.5\ H_2O$ (319.39): C 75.21, H 7.26; found: C 75.46, H 7.51.

*(1*S*,2*R*,4*S*,5*R*)-4-(Phenylmethoxy)-5-[(phenylmethoxy)methyl]bicyclo[3.1.0]hexan-2-ol* (**14a**). A stirred soln. of alcohol **18** (0.66 g, 2.15 mmol) in dry CH_2Cl_2 (30 ml) was cooled over an ice-salt bath. Then 1M diethyl zinc in hexane (2.4 ml) was added dropwise, and the reaction was allowed to continue for 0.25 h after the addition. Separately, a soln. of diiodomethane (0.4 ml, 4.74 mmol) in dry CH_2Cl_2 (10 ml) was prepared, and 5.2 ml of this soln. was added to the mixture. After 5 min stirring, an equal amount of diethylzinc was added dropwise, followed by the remaining soln. of diiodomethane (4.8 ml). The mixture was stirred for a total of 6 h, while the cooling bath gradually warmed to r.t. Then, the mixture was poured into an aq. sat. NH_4Cl soln. (50 ml), and extracted with CH_2Cl_2 (3 × 50 ml). The combined extract was washed with sat. NH_4Cl soln. (2 × 50 ml), dried ($MgSO_4$), and evaporated, and the residue purified by FC (silica gel, step gradient of 25% and 50% AcOEt/hexanes): **14a** (0.560 g, 80%). Oil. ^{1}H-NMR ($CDCl_3$): 7.45–7.30 (*m*, 2 Ph); 4.65–4.40 (*m*, 2 PhCH_2O, H–C(4)); 4.31 (*t*, *J* = 8.0, H–C(2)); 3.98 (*d*, *J* = 10.5, 1 H, PhCH_2OCH_2); 3.21 (*d*, *J* = 10.5, 1 H, PhCH_2OCH_2); 2.37 (*dt*, *J* = 12.9, 7.4, H_a–C(3)); 1.70–1.60 (*m*, OH, H–C(3)); 1.40–1.20 (*m*, H–C(1), H_a–C(6)); 0.63 (*dd*, *J* = 7.4, 5.6, H_b–C(6)). ^{13}C-NMR ($CDCl_3$): 138.84; 138.53; 128.49; 128.47; 127.88; 127.78; 127.72; 127.70; 73.01; 72.13; 71.87; 70.02; 35.59; 32.99; 28.20; 7.00. Anal. calc. for $C_{21}H_{24}O_3$ (324.41): C 77.74, H 7.46; found: C 77.51, H 7.40.

*(1*R*,2*S*,4*S*,5*S*)-4-(6-Amino-9*H*-purin-9-yl)-2-hydroxybicyclo[3.1.0]hexan-1-methanol* (**8**). Diethyl azodicarboxylate (DEAD; 0.63 ml, 3.98 mmol) was added dropwise to a soln. of Ph_3P (1.04 g, 3.98 mmol) in dry THF (8.5 ml) previously cooled in an ice-salt bath. After 20 min, this soln. was added dropwise to a soln. of **14a** (0.560 g, 1.73 mmol) and 6-chloro-1*H*-purine (0.431 g, 2.77 mmol) in dry THF (8.5 ml), which was also cooled in an ice-salt bath. The mixture was stirred cold for 0.5 h and then at r.t. for 3 h. The volatiles were removed and the residue purified by FC (silica gel, 25% AcOEt/hexanes): *6-chloro-9-{(1*S*,2*S*,4*S*,5*R*)-4-(phenylmethoxy)-5-[(phenylmethoxy)methyl]bicyclo[3.1.0]hex-2-yl}-9*H*-purine* (**19**; 0.741 g, 93%), slightly contaminated with DEAD. ^{1}H-NMR ($CDCl_3$): 9.20 (*s*, H–C(2)); 8.80 (*s*, H–C(8)); 7.50–7.30 (*m*, 2 Ph); 5.35 (*d*, *J* = 5.2, H–C(2′)); 4.75 (*t*, *J* = 8.5, H–C(4′)); 4.65 (br. *s*, PhCH_2O); 4.55 (*AB* (*m*), PhCH_2O); 4.30–4.50 (DEAD contamination); 4.25 (*d*, *J* = 9.9, 1 H, PhCH_2OCH_2); 3.25 (*d*, *J* = 9.9, 1 H, PhCH_2OCH_2); 2.15 (*m*, H_a–C(3′)); 1.95 (*m*, H_b–C(3′)); 1.80 (*m*, H–C(1′)); 1.45 (DEAD contamination); 1.25 (*m*, H_a–C(6′)); 0.95 (*m*, H_b–C(6′)).

Since the DEAD contamination was successfuly removed only after the final deprotection step, **19** (0.481 g, 1.04 mmol) was dissolved in a minimum amount of MeOH and added to a sat. NH_3/MeOH soln. (90 ml) in a sealed pressure steel bomb which was heated at 70° overnight. After cooling, the soln. was evaporated and co-evaporated twice with MeOH (100 ml) before purification by FC (silica gel, 2% MeOH/$CHCl_3$): *9-{(1*S*,2*S*,4*S*,5*R*)-4-(phenylmethoxy)-5-[(phenylmethoxy)methyl]bicyclo[3.1.0]hex-2-yl}-9*H*-purin-6-amine* (**20**; 0.347 g, 75%). Heavy syrup. ^{1}H-NMR ($CDCl_3$): 8.65 (*s*, H–C(2)); 8.40 (*s*, H–C(8)); 7.50–7.30 (*m*, 2 Ph); 6.75 (br. *s*, NH_2); 5.25 (*d*, *J* = 6.1, H–C(2′)); 4.75 (*t*, *J* = 8.2, H–C(4′)); 4.65 (br. *s*, PhCH_2O); 4.55 (*AB* (*m*), PhCH_2O); 4.15–4.35 (*m*, 1 H of PhCH_2OCH_2, DEAD contamination); 3.25 (*d*, *J* = 9.9, 1 H, PhCH_2OCH_2); 2.15 (*m*, H_a–C(3′)); 1.95 (*m*, H_b–C(3′)); 1.70 (*m*, H–C(1′)); 1.40 (DEAD contamination); 1.20 (*m*, H_a–C(6′)); 0.90 (*m*, H_b–C(6′)).

Compound **20** was used directly for the final deprotection step: A soln. of **20** (0.347 g, 0.787 mmol) in MeOH (96 ml) was treated with 96% formic acid (4 ml) and stirred overnight in the presence of Pd black (0.5 g). The insolubles were removed by filtration with the aid of *Celite*, and the filtrate was evaporated to give a white solid. To this solid, $CHCl_3$ (50 ml) was added and the mixture heated, cooled, and filtered. The remaining solid was recrystallized from MeOH/Et_2O: pure **8** (0.160 g, 78%). Solid. M.p. 259–261° (dec.), identical to that of an authentic sample.

REFERENCES

[1] R. Wolfenden, J. Kaufman, J. B. Macon, *Biochemistry* **1969**, *8*, 2412.
[2] B. E. Evans, R. Wolfenden, *Biochemistry* **1973**, *12*, 392.
[3] For a review of ADA deficiency, see M. S. Hershfield, B. S. Mitchell, in 'The Metabolic and Molecular Basis of Inherited Disease', Ed. C. R. Scriver, A. L. Beaudet, W. S. Sly, D. Valle, McGraw Hill, New York, 1995, pp. 1725–1768.
[4] J. K. Lowe, B. Gowans, L. Brox, *Cancer Res.* **1977**, *37*, 3013.
[5] J. M. Wilson, B. S. Mitchell, P. E. Daddona, W. N. Kelley, *J. Clin. Invest.* **1979**, *64*, 1475.
[6] B. Evans, R. Wolfenden, *J. Am. Chem. Soc*. **1970**, *92*, 4751.
[7] M. Ohno, N. Yagisawa, S. Shibahara, S. Kondo, K. Maeda, H. Umezawa, *J. Am. Chem. Soc*. **1974**, *96*, 4326.
[8] H. Nakamura, G. Koyama, Y. Iitaka, M. Ohno, N. Yagisawa, S. Kondo, K. Maeda, H. Umezawa, *J. Am. Chem. Soc*. **1974**, *96*, 4327.
[9] P. W. K. Wood, H. W. Dion, S. M. Lange, L. F. Dahl, L. Durham, *J. Heterocycl. Chem*. **1974**, *11*, 641.
[10] S. Cha, R. P. Agarwal, R. E. Parks Jr., *Biochem. Pharmacol*. **1975**, *24*, 2187.
[11] W. M. Kati, S. A. Acheson, R. Wolfenden, *Biochemistry* **1992**, *31*, 7356.
[12] D. K. Wilson, F. B. Rudolph, F. A. Quiocho, *Science* (*Washington, D.C.*) **1991**, *252*, 1278.
[13] A. J. Sharf, D. K. Wilson, Z. Chang, F. A. Quiocho, *J. Mol. Biol*. **1992**, *226*, 917.
[14] Z. Wang, F. A. Quiocho, *Biochemistry* **1998**, *37*, 8314.
[15] M. D. Erion, M. R. Reddy, *J. Am. Chem. Soc*. **1998**, *120*, 3295.
[16] C. Altona, M. Sundaralingam, *J. Am. Chem. Soc*. **1972**, *94*, 8205.
[17] For a comprehensive review of these concepts, see W. Saenger, 'Principles of Nucleic Acid Structure', Springer-Verlag, New York, 1984.
[18] C. Thibaudeau, A. Kumar, S. Bekiroglu, A. Matsuda, V. E. Marquez, J. Chattopadhyaya, *J. Org. Chem*. **1998**, *63*, 5447.
[19] A. A. Koshkin, S. K. Singh, P. Nielsen, V. K. Rajwanshi, R. Kumar, M. Meldgaard, C. E. Olsen, J. Wengel, *Tetrahedron* **1998**, *54*, 3607.
[20] M. A. Siddiqui, H. Jr. Ford, C. George, V. E. Marquez, *Nucleosides Nucleotides* **1996**, *15*, 235.
[21] A. Ezzitouni, V. E. Marquez, *J. Chem. Soc., Perkin Trans. 1* **1997**, 1073.
[22] V. E. Marquez, P. Russ, R. Alonso, M. A. Siddiqui, K.-J. Shin, C. George, M. C. Nicklaus, F. Dai, H. Ford Jr., *Nucleosides Nucleotides* **1999**, *18*, 521.
[23] K. Biggadike, A. D. Borthwick, A. M. Exall, B. E. Kirk, S. M. Roberts, P. Youds, A. M. Z. Slawin, D. J. Williams, *J. Chem. Soc., Chem. Commun*. **1987**, 255.
[24] K. Biggadike, A. D. Borthwick, D. Evans, A. M. Exall, B. E. Kirk, S. M. Roberts, L. Stephenson, P. Youds, *J. Chem. Soc., Perkin Trans 1* **1988**, 549.
[25] A. Ezzitouni, P. Russ, V. E. Marquez, *J. Org. Chem.* **1997**, *62*, 4870.
[26] S. Obika, N. Daishu, Y. Hari, K.-I. Morio, Y. In, T. Ishida, T. Imanishi, *Tetrahedron Lett*. **1997**, *38*, 8735.
[27] C. Thibaudeau, J. Plavec, J. Chattopadhyaya, *J. Org. Chem*. **1996**, *61*, 266.
[28] For a comprehensive review of these concepts, see C. Thibaudeau, J. Chattopadhyaya, 'Stereoelectronic Effects in Nucleosides and Nucleotides and their Structural Implications', Uppsala University Press, Uppsala, Sweden, 1999.
[29] S. D. Lindell, B. A. Moloney, B. D. Hewit, C. G. Earnshaw, P. J. Dudfeld, J. E. Dancer, *Bioorg. Med. Chem. Lett*. **1999**, *9*, 1985.

Received August 23, 1999